

ROS accumulation and antiviral defence control by microRNA528 in rice

Jianguo Wu^{1,2†}, Rongxin Yang^{3†}, Zhirui Yang^{1†}, Shengze Yao¹, Shanshan Zhao¹, Yu Wang¹, Pingchuan Li⁴, Xianwei Song³, Lian Jin¹, Tong Zhou⁵, Ying Lan⁵, Lianhui Xie², Xueping Zhou⁶, Chengcai Chu³, Yijun Qi⁷, Xiaofeng Cao^{3,8*} and Yi Li^{1*}

MicroRNAs (miRNAs) are key regulators of plant–pathogen interactions. Modulating miRNA function has emerged as a new strategy to produce virus resistance traits^{1–5}. However, the miRNAs involved in antiviral defence and the underlying mechanisms remain largely elusive. We previously demonstrated that sequestration by Argonaute (AGO) proteins plays an important role in regulating miRNA function in antiviral defence pathways⁶. Here we reveal that cleavage-defective AGO18 complexes sequester microRNA528 (miR528) upon viral infection. We show that miR528 negatively regulates viral resistance in rice by cleaving *L-ascorbate oxidase (AO)* messenger RNA, thereby reducing AO-mediated accumulation of reactive oxygen species. Upon viral infection, miR528 becomes preferentially associated with AGO18, leading to elevated AO activity, higher basal reactive oxygen species accumulation and enhanced antiviral defence. Our findings reveal a mechanism in which antiviral defence is boosted through suppression of an miRNA that negatively regulates viral resistance. This mechanism could be manipulated to engineer virus-resistant crop plants.

RNA silencing plays crucial roles in plant antiviral defence responses by targeting viral genomes with small interfering RNAs, and by regulating the expression of key defence genes with microRNAs (miRNAs)^{1,4,7}. Accordingly, manipulating miRNA-mediated gene regulation has emerged as a new strategy to enhance pathogen defences in crop plants^{1,3,4}. However, the miRNAs involved in antiviral defence and the underlying mechanisms remain largely elusive. In this study, we used the rice (*Oryza sativa*)-rice stripe virus (RSV) pathosystem to establish that rice miR528 accommodates RSV infection and that the rice antiviral immune system suppresses this role of miR528 at multiple levels.

We previously showed that RSV infection caused miR528 to be sequestered by Argonaute (AGO) 18, a decoy AGO protein incapable of cleaving target RNAs⁶. miR528 has been found exclusively in monocots, and studies in several plant species indicate that it contributes to acclimation to abiotic stress^{8,9}. Our finding suggests that rice miR528 is involved in the RSV infection process. To test this, we obtained the rice T-DNA insertion mutant *mir528* (PFG_3A-11864.R) from the Korean RiceGE database and found that, in *mir528* plants, both primary miR528 (*pri-miR528*) and mature miR528, are undetectable¹⁰. The *mir528* mutant plants did not exhibit notable

developmental abnormalities at vegetative stages under normal growth conditions (Supplementary Fig. 1). In addition, we generated two transgenic rice lines, *mir528OE no. 1* and *mir528OE no. 2*, which overexpress miR528.

To test whether the changes in miR528 levels affected viral defence, the three rice lines with altered miR528 levels were inoculated with RSV-carrying brown planthopper (*Laodelphax striatellus*) and monitored for differences in viral disease progression. Compared to the parental *Dongjin* (DJ) rice, *mir528* mutant plants showed milder symptoms and lower infection rates. By contrast, *mir528OE* lines were more susceptible to RSV infection than their wild-type *Nipponbare* (NPB) parents (Supplementary Table 1 and Fig. 1a). These observations were confirmed by quantification of RSV genomic RNA levels by RNA blot analysis and quantitative PCR with reverse transcription (RT-qPCR). The levels of four of the RSV genome segments were substantially elevated in *mir528OE* lines, but drastically reduced in *mir528* plants (Fig. 1b). Further quantification by RT-qPCR confirmed that transcripts of the RSV-encoded CP gene were at least sevenfold more abundant in the *mir528OE* lines (compared to NPB controls), but ~50% lower in *mir528* lines (compared to DJ controls) (Fig. 1c). To confirm that miR528 deficiency is responsible for the altered resistance to RSV in *mir528* mutant plants, we restored the wild-type level of miR528 expression in the *mir528* mutant by transgenic expression of the *mir528com* construct. As expected, restoration of miR528 expression also restored RSV levels to those of wild-type plants (Supplementary Table 1 and Supplementary Fig. 2a,b). Therefore, regulation of miR528 levels contributes to the maintenance of basal resistance to RSV in wild-type rice plants.

To investigate how miR528 regulates basal antiviral resistance in rice, we tested whether potential miR528 targets have altered transcript levels in response to RSV infections, by mining previous RNA deep sequencing data (data not shown)^{11,12}. Four genes, including those encoding an L-ascorbate oxidase (AO), a plastocyanin-like protein, a RING-H2 finger E3 ubiquitin ligase known as VirE2-interacting protein 2¹³ and an F-box domain and leucine-rich repeat-containing protein known as DWARF3, were identified as putative miR528 targets based on perturbations in their transcript levels in response to altered miR528 levels in different rice lines. We further examined the expression of these genes by RT-qPCR in *mir528* knockout and miR528 overexpression lines with and

¹The State Key Laboratory of Protein and Plant Gene Research, College of Life Sciences, Peking University, Beijing 100871, China. ²State Key Laboratory of Ecological Pest Control for Fujian and Taiwan Crops, Fujian Province Key Laboratory of Plant Virology, Institute of Plant Virology, Fujian Agriculture and Forestry University, Fuzhou 350002, China. ³State Key Laboratory of Plant Genomics and National Center for Plant Gene Research, Institute of Genetics and Developmental Biology, Chinese Academy of Sciences, Beijing 100101, China. ⁴Agriculture and Agri-Food Canada, Morden, Manitoba R6M 1Y5, Canada. ⁵Institute of Plant Protection, Jiangsu Academy of Agricultural Sciences, Nanjing 210014, China. ⁶State Key Laboratory of Rice Biology, Institute of Biotechnology, Zhejiang University, Hangzhou 310029, China. ⁷Center for Plant Biology, Tsinghua-Peking Center for Life Sciences, College of Life Sciences, Tsinghua University, Beijing 100084, China. ⁸CAS Center for Excellence in Molecular Plant Sciences, Institute of Genetics and Developmental Biology, Chinese Academy of Sciences, Beijing 100101, China. [†]These authors contributed equally to this work. *e-mail: liyij@pku.edu.cn; xfcao@genetics.ac.cn

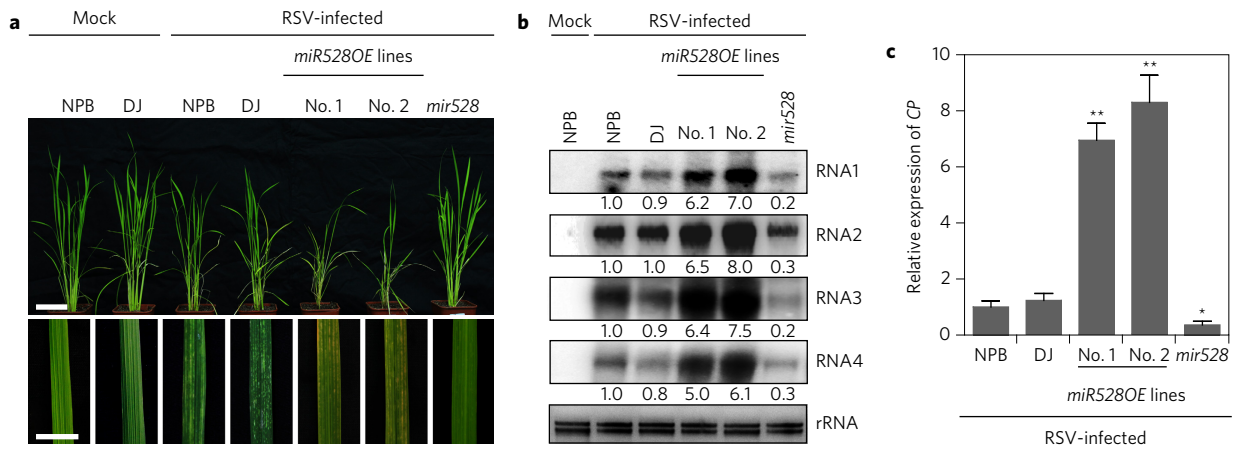


Figure 1 | MiR528 is required for antiviral immunity. **a**, Photographs of mock-inoculated or RSV-infected wild-type (NPB and DJ), miR528 overexpression (*miR528OE*; NPB background) and *mir528* (DJ background) plants. Scale bars, 10 cm (upper panel) and 5 cm (lower panel). **b**, Detection of the four RSV genomic RNA segments in the indicated plants by RNA blot analysis. Ribosomal RNAs (rRNAs) served as the loading control. Numbers beneath lanes indicate relative band intensities to quantify loading and are normalized for each panel (see Methods). **c**, Detection of expression levels of RSV CP in RSV-infected wild-type (NPB and DJ), *miR528OE* and *mir528* plants by RT-qPCR. The average values of three biological repeats are shown. Error bars represent standard deviations. Asterisks mark significant differences according to Student's *t*-test; **P* value ≤ 0.05 ; ***P* value ≤ 0.01 .

without RSV inoculation. Among these four genes, only *AO* was significantly induced by RSV infection. Interestingly, *AO* expression was inversely correlated with miR528 levels in various rice lines. Consistent with the idea that miR528 negatively regulates *AO* messenger RNA (mRNA), we found that *AO* protein levels were reduced in *miR528OE* lines but elevated in the *mir528* mutant line, and that RSV infection increased *AO* protein levels in all rice lines tested (Supplementary Fig. 3a,b). Together, these data suggest that *AO* is a strong candidate for a target gene of miR528 in its regulation of the rice immune response to RSV.

AO encodes one of ten rice AOs¹⁴. Phylogenetic analysis of *AO* genes from rice and *Arabidopsis* showed that *AO* is highly conserved in both monocots and dicots (Supplementary Fig. 4). *AO* localizes in the cell wall and catalyses apoplastic oxidation of L-ascorbic acid (AsA)^{15–17}. In agreement with our RT-qPCR and immunoblot results, the *miR528OE* lines and *mir528* mutant line had lower and higher *AO* enzymatic activities, respectively, compared to their NPB and DJ controls (Supplementary Fig. 3a–c). To verify that basal *AO* level was important for rice antiviral defence, we performed a time-course analysis of *AO* and RSV CP expression levels in wild-type and *mir528* mutant rice plants. We found that *AO* and CP expression gradually increased from 0 to 7 days post-inoculation and accumulated during RSV infection in wild-type plants (Supplementary Fig. 3d blue lines). By contrast, in *mir528* mutant plants, the transcript levels of *AO* and CP exhibited opposite patterns: *AO* was several-fold higher, but CP was much lower than that of wild-type plants, and both *AO* and CP maintained these levels from 0 to 14 days post-inoculation (Supplementary Fig. 3d green lines). These results suggest that the resistance of *mir528* plants depends on basal elevated *AO* levels in the early infection stage.

The target site of miR528 in the *AO* mRNA resides in the 3' untranslated region. We produced a miR528-resistant *AO* genomic DNA by mutating the miR528 target site, and generated transgenic rice plants that express the miR528-resistant *AO* mRNA under the control of *AO* native promoter (*pAO:AO Res*) (Fig. 2a). Transgenic plants expressing a wild-type *AO* (*pAO:AO*) were also generated to serve as controls. The levels of *AO* mRNA, protein and enzymatic activity were all much higher in the *pAO:AO Res* lines than in NPB and *pAO:AO* lines (Fig. 2b–d and Supplementary Fig. 5). These results demonstrate that *AO* mRNA is a direct target of miR528.

To investigate the role of *AO* in plant antiviral defence responses to RSV infection, we then tested the effect of *AO* overaccumulation

on plant antiviral capabilities. We found that the infection rates in the *pAO:AO Res* lines were lower than that in the wild-type NPB plants and the *pAO:AO* lines (Supplementary Table 1). Additionally, RSV-infected *pAO:AO Res* lines exhibited milder disease symptoms and less abundance of the viral genomic RNAs when compared with RSV-infected NPB plants and the RSV-infected *pAO:AO* lines (Fig. 2e,f). We conclude from these results that *AO* plays a positive role in plant defence against RSV.

Earlier studies reported that *AO* regulates the redox state of the apoplast by oxidizing apoplastic AsA, rendering it less effective at detoxifying reactive oxygen species (ROS)^{16,18–21}. The ROS burst in response to abiotic or biotic stresses has protective roles, as evidenced by studies showing that some ROS function as secondary messengers of signal transduction pathways controlling pathogen defence responses^{19,22,23}. However, excessive ROS causes serious damage; thus, plants and animals tightly regulate ROS production and detoxification^{17,23}. Based on these reports, we hypothesize that, through miR528 sequestration, rice plants respond to RSV invasion by upregulating *AO* activity, which in turn oxidizes AsA and decelerates ROS detoxification, permitting ROS to exert their role in antiviral defence. Consistent with our hypothesis, a previous study showed that overexpression of rice miR528 in creeping bentgrass (*Agrostis stolonifera* L.) correlated with reduced *AO* expression and accelerated ROS detoxification⁹. Conversely, *AO* overexpression in *Nicotiana tabacum* (tobacco) enhanced ROS accumulation and thereby sensitized plants to ozone stress^{16,21}.

To test our hypothesis, we first assessed whether elevated *AO* activity in *mir528* mutant and *pAO:AO Res* transgenic plants altered the levels of AsA and its oxidation product dehydroascorbate. A previous report defined the redox status as the ratio of AsA to total ascorbate (AsA + dehydroascorbate)¹⁴, with a higher value indicating a more robust redox system. Our results (Fig. 3a,b) indicated that this ratio was higher in *miR528OE* lines, but significantly lower in *mir528* mutants and *pAO:AO Res* lines than in NPB and DJ lines, indicating that the redox activity and AsA levels are inversely correlated with *AO* levels (Fig. 3b,c). We then determined basal ROS levels in different rice lines not infected with RSV under normal growth conditions by monitoring the accumulation of superoxide (O_2^-) and hydrogen peroxide (H_2O_2). Nitroblue tetrazolium (NBT) staining for O_2^- and 3,3'-diaminobenzidine (DAB) staining for H_2O_2 showed that ROS accumulated to higher levels in *mir528*

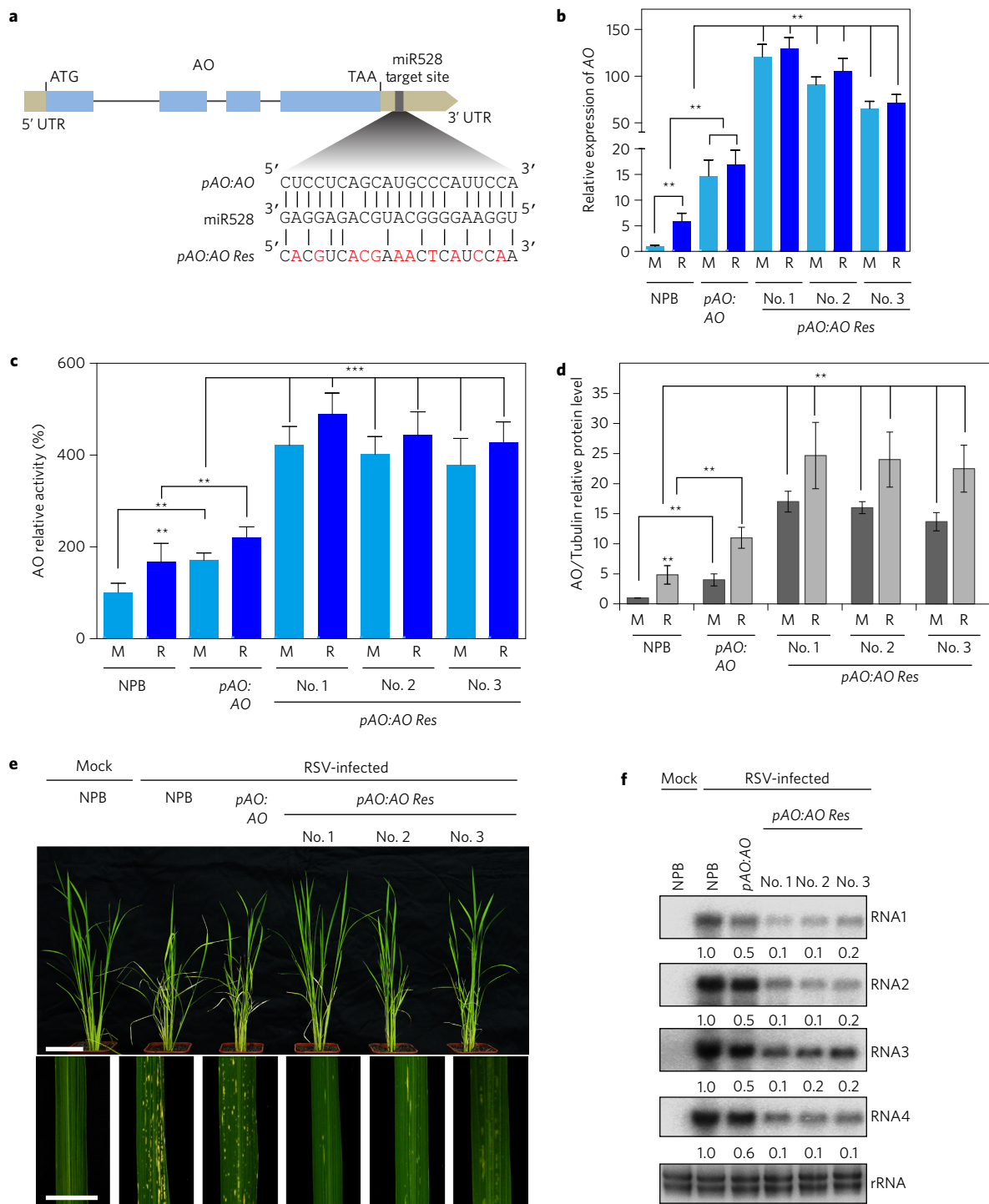


Figure 2 | Transgenic expression of miR528-resistant AO mRNA-enhanced virus resistance in rice. **a**, Schematic diagram of AO showing the target site of miR528. In AO that is resistant to miR528 cleavage (AO Res), 11 nucleotide substitutions were introduced into the miR528 target site. **b**, RT-qPCR analysis of AO expression levels in mock (M) or RSV-inoculated (R) NPB and transgenic plants expressing pAO:AO or AO Res in the NPB background. Expression levels were normalized using the signal from *OsEF-1a*. The average values of three biological repeats are shown. Error bars represent standard deviations. Asterisks mark significant differences according to Student's *t*-test; ***P* value ≤ 0.01 . **c**, Relative AO activity in NPB and transgenic plants expressing pAO:AO or AO Res in the NPB background. Values are means of three biological replicates. Error bars indicate standard deviations. Asterisks mark significant differences according to Student's *t*-test; ***P* value ≤ 0.01 ; ****P* value ≤ 0.001 . **d**, Quantification of relative AO/tubulin protein levels from NPB, pAO:AO and pAO:AO Res lines infected or not infected with RSV. Corresponds to Supplementary Fig. 5. Error bars represent standard deviations of triplicate experiments. Asterisks mark significant differences in relative AO/tubulin protein levels according to Student's *t*-test; ***P* value ≤ 0.01 . **e**, Symptoms of mock- or RSV-inoculated NPB plants and transgenic plants expressing pAO:AO and AO Res. Scale bars, 10 cm (upper panel) and 5 cm (lower panel). **f**, Detection of RSV genomic RNA segments in the indicated plants by RNA blot analysis. The blots were hybridized with radiolabelled riboprobes specific for each RNA segment. Ribosomal RNAs were stained with ethidium bromide and served as the loading control. The RNA signals were quantified and normalized to rRNAs, and the relative values were calculated by comparison with those in RSV-infected NPB (arbitrarily set to 1.0).

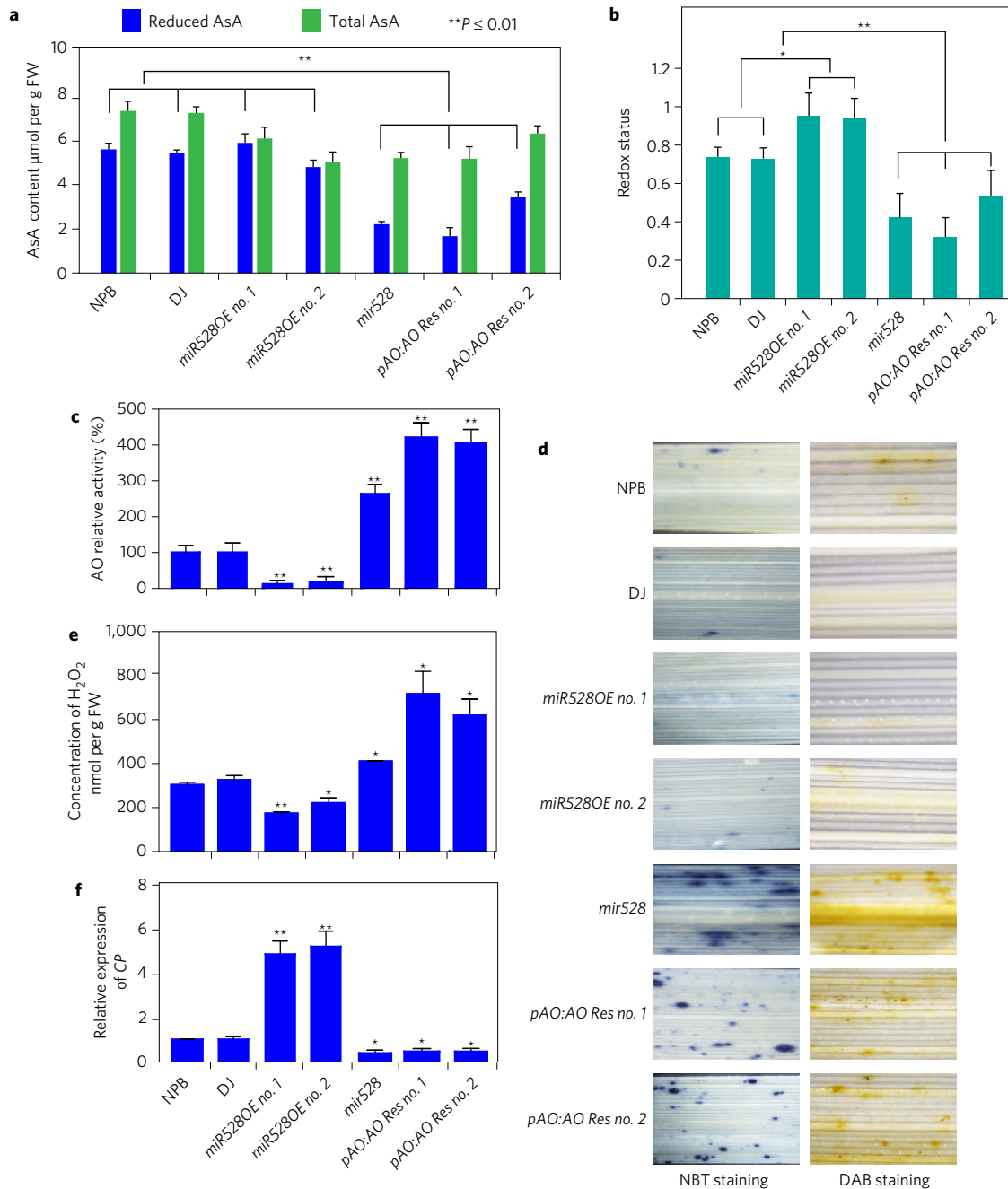


Figure 3 | AO enhanced accumulation of ROS in rice. **a**, L-ascorbic acid (AsA) characteristics in whole leaf tissue of the indicated plant lines. Values are the means of three biological replicates. Error bars indicate standard deviations. Asterisks mark significant differences in reduced AsA levels according to Student's *t*-test; ** P value ≤ 0.01 . FW, fresh weight. **b**, Redox status was defined as the amount of AsA divided by the total ascorbate amount (AsA+ dehydroascorbate). Values are the means of three biological replicates. Error bars indicate standard deviations. Asterisks mark significant differences in redox status according to Student's *t*-test; * P value ≤ 0.05 ; ** P value ≤ 0.01 . **c**, Relative AO activity in the healthy indicated plants compared with wild-type plants. Values are the means of three biological replicates. Error bars indicate standard deviations. Asterisks mark significant differences according to Student's *t*-test; ** P value ≤ 0.01 . **d**, *In situ* detection of leaf ROS levels using DAB and NBT staining in the healthy indicated rice plants. **e**, Quantification of H_2O_2 levels in four-week-old plants of the indicated lines. Results are the means of three biological replicates. Error bars indicate standard deviations. Asterisks mark significant differences according to Student's *t*-test; * P value ≤ 0.05 ; ** P value ≤ 0.01 . **f**, Detection of RSV CP levels in the indicated rice plants infected with RSV, by quantitative RT-qPCR. The average values of three biological repeats are shown. Error bars represent standard deviations. Asterisks mark significant differences according to Student's *t*-test; * P value ≤ 0.05 ; ** P value ≤ 0.01 .

mutant and *pAO:AO Res* lines that contained less AsA (Fig. 3d). Quantification of H_2O_2 in indicated rice seedlings also showed that H_2O_2 accumulated in both *mir528* mutants and *pAO:AO Res* transgenic lines (Fig. 3e). Together, these data confirm a direct role of AO in regulating basal ROS levels in rice through its action on AsA. To determine whether higher basal ROS levels correlate with

enhanced antiviral immunity, we evaluated RSV CP RNA levels in various rice lines with different basal ROS levels. Strikingly, lines with higher basal ROS levels, including *mir528* and *pAO:AO Res*, accumulated less viral CP RNA, whereas plants with lower basal ROS levels expressed higher levels of viral CP RNA (Fig. 3f). In addition, to distinguish the function of basal ROS levels from virus

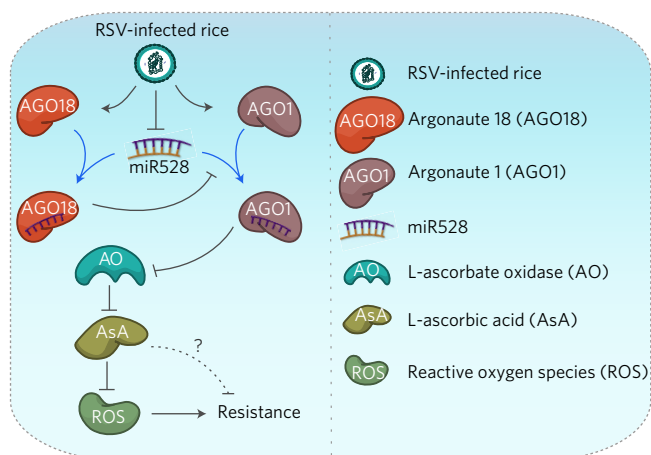


Figure 4 | A model of miRNA528 function in regulating plant antiviral immunity. In rice infected with RSV, miR528 is suppressed at both the transcriptional and post-transcriptional levels. First, RSV infection decreases miR528 expression and induces the accumulation of AGO18 and AGO1. Then, AGO18 sequesters miR528 away from AGO1 to block the formation of an effective RNA-induced silencing complex. These events induce the accumulation of the miR528 target AO, which catalyses AsA oxidation, thereby regulating the redox status and priming ROS-mediated resistance against RSV infection. Solid lines represent regulatory links observed in rice, and dashed lines represent regulatory links observed in *Arabidopsis* and other plants. Arrows indicate positive regulation and blunt-ended bars indicate inhibition. Blue arrows indicate AGOs binding miR528. A line does not necessarily represent unique or direct regulation. A question mark refers to unverified regulation upon virus infection.

infection-induced ROS, we determined the O_2^- and H_2O_2 levels in RSV-infected rice plants through NBT and DAB staining, respectively. ROS accumulated to high levels in the *mir528OE* lines and wild-type rice but accumulated to low levels in the *mir528* mutants and *pAO:AO Res* lines (Supplementary Fig. 6). These data indicate that successful virus infection can cause much higher ROS accumulation, leading to cell death and damage to host plants. In summary, our findings demonstrate that AO enhances basal ROS-mediated resistance to RSV by oxidizing AsA, the primary ROS scavenger (Fig. 4).

To determine whether AO-induced ROS accumulation is a general mechanism by which rice resist viral pathogens, we used another typical plant virus system, *Rice black streaked dwarf virus* (RBSDV), a double-stranded RNA virus that infects different plant hosts, including rice and *Zea mays* (maize), to test the antiviral function of the indicated rice lines. We found that the *mir528OE* lines exhibited much more severe disease symptoms and higher infection rates than the *mir528* mutants and *pAO:AO Res* lines (Supplementary Table 3). RT-qPCR analysis of the accumulation of different RNA genome fragments of RBSDV showed that the levels of RBSDV RNA are consistent with the visible disease symptoms. We then measured the AO mRNA levels and AO enzyme activities of both RBSDV-infected and mock-inoculated rice lines and found that AO transcript levels and AO enzymatic activity were much higher in *mir528* and *pAO:AO Res* lines than in *mir528OE* lines (Supplementary Fig. 7). Together, these data suggest that AO-induced ROS accumulation has broad functions in antiviral defence in plants.

We next investigated how miR528 expression is regulated in rice upon virus attack. We previously found that miR528 levels were downregulated by RSV infection²⁴. This observation was confirmed by RNA blot analysis, which showed that the level of the 21-nucleotide mature miR528 was reduced by ~30% in RSV-infected plants. To determine whether lower miR528 accumulation was caused by downregulation of transcription of the miR528 precursor, we

analysed the expression level of miR528 precursor (*pre-miR528*) by RT-qPCR. Our results showed that the level of *pre-miR528* decreased by 50% upon RSV infection (Supplementary Fig. 8a,b). Further experiments with transgenic rice that express β -glucuronidase under the control of the *miR528* native promoter indicated that RSV infection resulted in decreased transcription of the *miR528* promoter (Supplementary Fig. 8c,d). Therefore, in addition to AGO18-mediated sequestration, RSV infection caused transcriptional downregulation of *miR528*. Furthermore, RNA blot analysis showed that RSV infection induced the accumulation of 20-nucleotide tandem or random miR528. To exclude the function of these miRNAs in the plant's response to RSV infection, we analysed their sequences and identified the most enriched sequence (Supplementary Fig. 8e). AGO complex immunoprecipitation-sequencing data from previous studies confirmed that this 20-nucleotide miR528 associated with AGO18⁶.

To confirm the preferential association of miR528 with AGO18 upon RSV attack, we tested whether AGO18 indeed competes with AGO1 for the binding of miR528. We transiently expressed a miR528 precursor together with either *Flag-AGO1a* or *Flag-AGO1b* in the presence and absence of *Myc-AGO18*, respectively. Expression of *Myc-AGO18* caused a reduction of miR528 in the AGO1a and AGO1b complexes, and a concurrent increase of its association with the AGO18 complex (Supplementary Fig. 9). These data demonstrate that AGO18 effectively competes with AGO1 for miR528 binding⁶. More importantly, RSV infection also enhanced the expression of AGO18, which is expected to enhance its sequestration of miR528, further diminishing the miR528 fraction available for AO degradation. Taken together, these results show that rice plants use a three-pronged strategy to ensure that AO functions effectively in antiviral defence, involving the transcriptional downregulation of miR528, transcriptional up-regulation of AGO18 and AGO18-mediated sequestration of miR528 (Fig. 4). It will be interesting to establish whether AO itself is also transcriptionally upregulated by viral infection.

Some AGOs, as exemplified by *Arabidopsis* AGO10 and rice AGO18, act as miRNA sinks that prevent certain miRNAs from associating with cleavage-active AGOs, thus adding another layer of fine-tuning of the RNA silencing functions^{6,25}. We previously showed that rice AGO18 sequesters the AGO1-targeting miR168 to increase the available AGO1 for antiviral RNA silencing. In the current study, we describe another novel contribution of AGO18 to antiviral defence in rice that involves sequestering the AO-targeting miR528, thus promoting the role of AO in enhancing antiviral defence response through regulation of ROS accumulation. To test whether crosstalk exists between these two pathways, we tested the expression patterns of miR168, *AGO1a*, *AGO1b* and *AGO18* in *mir528OE* and *mir528* mutant lines. We found no significant differences in expression among these plant lines (Supplementary Fig. 10a,b). These results suggest that miR528 deficiency and AO-mediated plant antiviral defence function in parallel with the AGO18-miR168-AGO1 pathway. We also measured the transcript levels of AO in both RSV-infected and mock-inoculated wild-type (NPB) and *ago18* mutant rice plants. AO mRNA accumulated to a lesser extent in RSV-infected *ago18* mutants than in NPB (Supplementary Fig. 10c), indicating that AO mRNA accumulation in RSV-infected plants requires AGO18. Although the exact functional mode of ROS in antiviral defence remains to be elucidated, it is well known that ROS are central players in the cellular signalling network in different organisms¹⁹. To summarize, our study not only reveals a pathway that elegantly regulates the availability of a key defence factor (AO) based on the sensing of virus attack, but also provides strong evidence to support that ROS have an active role in antiviral immunity. We foresee that this unique mechanism could be engineered to improve the antiviral capabilities of crops.

Methods

Plant growth and virus inoculation. All of the rice seeds came from Xiaofeng Cao's laboratory at the State Key Laboratory of Plant Genomics and National Center For Plant Gene Research, Institute of Genetics and Developmental Biology, Chinese Academy of Sciences. Plant growth and virus inoculation were essentially carried out as described in Du *et al.*²⁴ and Wu *et al.*⁶. Briefly, rice (*Oryza sativa* spp. *japonica*) seedlings were grown in a greenhouse at 28–30 °C and 60 ± 5% relative humidity under natural sunlight for 10 days. The viruliferous (RSV- and RBSDV-carrying) insects of *Laodelphax striatellus* and virus-free *Laodelphax striatellus* (mock) were used for inoculation. After feeding for 3 days, the insects were removed and the rice seedlings were returned to the greenhouse to grow under the greenhouse conditions above. After 3 weeks post-inoculation, when the newly developed leaves started to display viral symptoms, the whole seedlings were harvested. For each sample, at least 15 rice seedlings were pooled for RNA extractions.

Histochemical β -glucuronidase staining. Plants were infiltrated with 50 mM sodium phosphate (pH 7.0), 10 mM EDTA and 0.5 mg per ml X-gluc (Apollo Scientific), followed by incubation at 37 °C in the dark overnight and then destaining in 70% ethanol before photographing⁶.

Histochemical staining of O₂⁻ and H₂O₂. The histochemical staining of H₂O₂ and O₂⁻ were performed using DAB and NBT. Details of the procedures were described previously²⁶. Briefly, rice leaves were cut into 1 cm lengths and were infiltrated with 10 mM Tris-HCl (pH 6.5) containing 1 mg per ml DAB (Sigma) or 50 mM sodium phosphate (pH 7.0) containing 0.05% NBT (Sigma) and 10 mM Na₂S₂O₃, respectively, followed by incubation at 37 °C in the dark for 16 h. Then the leaves were washed with bleaching solution (ethanol:acetic acid = 3:1) to bleach out the chlorophyll at 70 °C for 30 min. Finally, the leaves were photographed using a stereoscope under uniform lighting.

AsA measurement assay. Extraction and quantification of AsA were based on Ueda *et al.*¹⁴. One hundred milligrams of rice sample materials were collected and ground with a mortar and pestle in liquid nitrogen. Total AsA was extracted with 1 ml extraction solvent (6% MPA) by centrifugation for 20 min at 4 °C and 15,000g. The reduced AsA content was measured from the absorption decrease at 265 nm after the addition of 10 μ l of 0.01 units per ml AO to a mixture of 10 μ l of extracted AsA and 80 μ l of 100 mM potassium phosphate buffer (pH 7.0). The oxidized AsA content was measured from the absorption increase at 265 nm after the addition of 10 μ l of 4 mM dithiothreitol to a mixture of 10 μ l of extracted AsA and 80 μ l of 100 mM potassium phosphate buffer (pH 7.8). The calculation of the AsA content was based on the extinction coefficient of (ϵ) = 14.3 mM⁻¹ cm⁻¹. All analyses were conducted at least in triplicate.

AO activity assay. AO activity was measured according to Ueda *et al.*¹⁴ and Pignocchi *et al.*¹⁵. One hundred milligrams of rice materials were collected and powdered in liquid nitrogen and then homogenized with 1 ml, 100 mM sodium phosphate (pH 6.5). The extracts were centrifuged at 15,000g for 10 min at 4 °C and soluble AO activity was measured on the supernatant. The assay mixture consisted of 10 μ l of the enzyme extract, 80 μ l of 100 mM sodium phosphate buffer (pH 5.6) and 10 μ l of 2 mM reduced AsA. The microplate was shaken to mix the solution and the kinetics were read at 265 nm (extinction coefficient (ϵ) = 14.3 mM⁻¹ cm⁻¹) with a microplate reader (Thermo Scientific Microplate Reader). The calculated results were relative activities compared to wild-type plants.

H₂O₂ determination. H₂O₂ was measured in extracts from indicated rice seedlings. Briefly, 100 mg of fresh rice leaves were harvested and ground to a fine powder with liquid nitrogen. The powder was extracted with 1 ml 50 mM sodium phosphate (pH 7.4) and incubated on ice for 20 min. The extracts were then centrifuged at 12,000g for 20 min at 4 °C. The concentration of H₂O₂ in the extracts was assayed using the Amplex Red Hydrogen Peroxide/Peroxidase Assay kit (Invitrogen molecular probe, catalogue number: A22188) following the manufacturer's directions. The absorbance was measured at ~560 nm using the microplate reader (Thermo Scientific Microplate Reader) and the amount of H₂O₂ was calculated according to the standard curve prepared with known concentrations of H₂O₂.

Generation of antibodies against rice AO. Synthetic peptides of AO (CDSPEQPEFRHQYDD) were used to raise rabbit polyclonal antibodies against AO, essentially as described¹². The antisera were affinity-purified and used for western blotting.

Purification of rice AGO-containing complexes; bioinformatics analysis of small RNA data sets and northern blotting. Assays of purification of rice AGO-containing complexes and bioinformatics analysis of small RNA data reference to Wu *et al.*⁶. Northern blot analysis was performed as described before⁶. ³²P-end labelled oligonucleotide probes complementary to small RNAs were used for northern blots. The sequences of the probes and primers are listed in Supplementary Table 2.

Western blotting. Protein samples were boiled with the same volume of 2×protein loading buffer at 95 °C for 5 min and separated by SDS-PAGE. Proteins were then

transferred to PVDF membranes and detected with antibodies against AO, Myc (11667203001, Roche), Flag (F1804, Sigma-Aldrich) and tubulin (T5168, Sigma-Aldrich).

Immunoblot quantification analysis. Quantification of immunoblots was conducted according to Saijo *et al.*²⁷ and Zheng *et al.*²⁸. Briefly, for western blot, band intensities of AO, tubulin (loading control for total lysates), Flag (AGO1a/b) or Myc (AGO18) were measured with ImageJ (<http://rsb.info.nih.gov/ij/>). Relative band intensities were then calculated using the ratio of AO/Tubulin for each immunoblot. For northern blot, band intensities of different RNA strands or miRNAs were also measured with ImageJ. Relative band intensities were then calculated through normalizing the first band or the band from wild-type as 1.0. All immunoblot experiments were repeated at least three times, essentially with the same conclusions, and representative results are shown.

Data availability. The data that support the findings of this study are available from the corresponding author on request.

Received 2 February 2016; accepted 23 November 2016;
published 6 January 2017

References

- Ruiz-Ferrer, V. & Voinnet, O. Roles of plant small RNAs in biotic stress responses. *Annu. Rev. Plant Biol.* **60**, 485–510 (2009).
- Katiyar-Agarwal, S. & Jin, H. Role of small RNAs in host-microbe interactions. *Annu. Rev. Phytopathol.* **48**, 225–246 (2010).
- Pedersen, I. M. *et al.* Interferon modulation of cellular microRNAs as an antiviral mechanism. *Nature* **449**, 919–922 (2007).
- Ding, S. W. & Voinnet, O. Antiviral immunity directed by small RNAs. *Cell* **130**, 413–426 (2007).
- Chen, X. Small RNAs and their roles in plant development. *Annu. Rev. Cell Dev. Biol.* **25**, 21–44 (2009).
- Wu, J. *et al.* Viral-inducible Argonaute18 confers broad-spectrum virus resistance in rice by sequestering a host microRNA. *eLife* **4**, e05733 (2015).
- Lindsay, M. A. microRNAs and the immune response. *Trends Immunol.* **29**, 343–351 (2008).
- de Lima, J. C., Loss-Morais, G. & Margis, R. MicroRNAs play critical roles during plant development and in response to abiotic stresses. *Genet. Mol. Biol.* **35**, 1069–1077 (2012).
- Yuan, S. *et al.* Constitutive expression of rice *MicroRNA528* alters plant development and enhances tolerance to salinity stress and nitrogen starvation in creeping bentgrass. *Plant Physiol.* **169**, 576–593 (2015).
- Jeon, J. S. *et al.* T-DNA insertional mutagenesis for functional genomics in rice. *Plant J.* **22**, 561–570 (2000).
- Zhou, M. *et al.* Degradome sequencing reveals endogenous small RNA targets in rice (*Oryza sativa* L. ssp. *indica*). *Front. Biol.* **5**, 67–90 (2010).
- Wu, L. *et al.* Rice MicroRNA effector complexes and targets. *Plant Cell* **21**, 3421–3435 (2009).
- Liu, L. *et al.* OsRFP2-10, a ring-H2 finger E3 ubiquitin ligase, is involved in rice antiviral defense in the early stages of rice dwarf virus infection. *Mol. Plant* **7**, 1057–1060 (2014).
- Ueda, Y., Siddique, S. & Frei, M. A novel gene, *OZONE-RESPONSIVE APOPLASTIC PROTEIN1*, enhances cell death in ozone stress in rice. *Plant Physiol.* **169**, 873–889 (2015).
- Pignocchi, C., Fletcher, J. M., Wilkinson, J. E., Barnes, J. D. & Foyer, C. H. The function of ascorbate oxidase in tobacco. *Plant Physiol.* **132**, 1631–1641 (2003).
- Pignocchi, C. *et al.* Ascorbate oxidase-dependent changes in the redox state of the apoplast modulate gene transcript accumulation leading to modified hormone signaling and orchestration of defense processes in tobacco. *Plant Physiol.* **141**, 423–435 (2006).
- Munne-Bosch, S., Queval, G. & Foyer, C. H. The impact of global change factors on redox signaling underpinning stress tolerance. *Plant Physiol.* **161**, 5–19 (2013).
- Brynildsen, M. P., Winkler, J. A., Spina, C. S., MacDonald, I. C. & Collins, J. J. Potentiating antibacterial activity by predictably enhancing endogenous microbial ROS production. *Nat. Biotechnol.* **31**, 160–165 (2013).
- Mittler, R. *et al.* ROS signaling: the new wave? *Trends Plant Sci.* **16**, 300–309 (2011).
- Venkatesh, J. & Park, S. W. Role of L-ascorbate in alleviating abiotic stresses in crop plants. *Bot. Stud.* **55**, 1–19 (2014).
- Asensi-Fabado, M. A. & Munne-Bosch, S. Vitamins in plants: occurrence, biosynthesis and antioxidant function. *Trends Plant Sci.* **15**, 582–592 (2010).
- Apel, K. & Hirt, H. Reactive oxygen species: metabolism, oxidative stress, and signal transduction. *Annu. Rev. Plant Biol.* **55**, 373–399 (2004).
- Mukherjee, M. *et al.* Ascorbic acid deficiency in *Arabidopsis* induces constitutive priming that is dependent on hydrogen peroxide, salicylic acid, and the *NPR1* gene. *Mol. Plant Microbe Interact.* **23**, 340–351 (2010).
- Du, P. *et al.* Viral infection induces expression of novel phased microRNAs from conserved cellular microRNA precursors. *PLoS Pathog.* **7**, e1002176 (2011).

25. Zhu, H. *et al.* *Arabidopsis* Argonaute10 specifically sequesters miR166/165 to regulate shoot apical meristem development. *Cell* **145**, 242–256 (2011).
26. Xia, X. J. *et al.* Reactive oxygen species are involved in brassinosteroid-induced stress tolerance in cucumber. *Plant Physiol.* **150**, 801–814 (2009).
27. Saijo, Y. *et al.* *Arabidopsis* COP1/SPA1 complex and FHY1/FHY3 associate with distinct phosphorylated forms of phytochrome A in balancing light signaling. *Mol. Cell* **31**, 607–613 (2008).
28. Zheng, X. *et al.* *Arabidopsis* phytochrome B promotes SPA1 nuclear accumulation to repress photomorphogenesis under far-red light. *Plant Cell* **25**, 115–133 (2013).

Acknowledgements

We thank F. Qu (Ohio State University) and Y. Li (Tsinghua-Peking Center for Life Sciences) for critical reading of the manuscript, L. Li (Peking University) for technical assistance, G. Liu (Tsinghua University) for assistance with the AO and AsA assay and the Integrated R & D Services – WuXi AppTec for generating the antisera used in this study. This work was supported by grants from the National Basic Research Program 973 (2014CB138400), Natural Science Foundation of China (91540203, 31530062, 31420103904, 31123007 and 31272018), the National Key Research and Development Program of China (2016YFD0100904), the Transgenic Research Program (2016ZX08010-001 and 2016ZX08009001-005) and state key laboratories of protein and plant gene research,

plant genomics. J.W. was supported in part by the Postdoctoral Fellowship of Peking-Tsinghua Center for Life Sciences.

Author contributions

J.W., Z.Y., X.C. and Y. Li designed the experiments; J.W., Z.Y., R.Y., Z.Y., S.Z., Y.W., L.J., P. L., X.S., T.Z. and Y. Lan performed the experiments; J.W., Z.Y., R.Y., L.X., X.Z., C.C., Y.Q., X. C. and Y. Li analysed the data; J.W., Z.Y. and Y. Li wrote the paper. All the authors discussed the results and commented on the manuscript.

Additional information

Supplementary information is available for this paper.

Reprints and permissions information is available at www.nature.com/reprints.

Correspondence and requests for materials should be addressed to X.C. and Y. Li.

How to cite this article: Wu, J. *et al.* ROS accumulation and antiviral defence control by microRNA528 in rice. *Nat. Plants* **3**, 16203 (2017).

Competing interests

The authors declare no competing financial interests.